Avoiding blindness in baryon number violating processes: Free-beam and intranuclear paths to neutron-antineutron transitions

Citation for the original published paper (version of record):
Barrow, J., Fierlinger, P., Kamyshkov, Y. et al (2026). Avoiding blindness in baryon number violating processes: Free-beam and intranuclear paths to neutron-antineutron transitions. Physical Review D, 113(9). http://dx.doi.org/10.1103/4p9z-nd1s

(article starts on next page)

Avoiding blindness in baryon number violating processes: Free-beam and intranuclear paths to neutron-antineutron transitions

Joshua L. Barrow,[1] Peter Fierlinger,[2] Yuri Kamyshkov,[3] Bernhard Meirose,[4,5] David Milstead,[6,7] Rabindra N. Mohapatra,[8] and Valentina Santoro[5,9]

[1]*School of Physics and Astronomy, The University of Minnesota, Twin Cities, Minneapolis, Minnesota 55455, USA*
[2]*Physik-Department, Technische Universität München, 85748 Garching, Germany*
[3]*Department of Physics and Astronomy, University of Tennessee, Knoxville, Tennessee 37996, USA*
[4]*Institutionen för Fysik, Chalmers Tekniska Högskola, Sweden*
[5]*Department of Physics, Lund University, 221 00 Lund, Sweden*
[6]*Department of Physics, Stockholm University, SE-106 91 Stockholm, Sweden*
[7]*Oskar Klein Centre, Stockholm, Sweden*
[8]*Department of Physics, University of Maryland, College Park, Maryland 20742, USA*
[9]*European Spallation Source ERIC, 221 00 Lund, Sweden*

(Received 20 December 2025; accepted 1 May 2026; published 28 May 2026)

Experimental searches for neutron-antineutron ($n \to \bar{n}$) transitions can be considered via two approaches: conversion in free-neutron beams and intranuclear transformation leading to matter instability in large-mass detectors. Plans for next-generation searches make it timely to highlight the complementarity, necessity, and limitations of each method. Converting the bound neutron limit into one for free neutrons traditionally utilizes nucleus-specific estimates of the in-medium suppression of $n \to \bar{n}$, obtained within mean-field theory under a single-operator assumption. This paper highlights how this suppression can be scenario-dependent, which can lead to deviations from the standard approach that can span several orders of magnitude. A further goal of the paper is to point out the need for a broader phenomenology program for $n \to \bar{n}$ that is akin to those developed for electric dipole moments and other systems for which short-distance new physics must be studied in medium. We find that moderate deviations from the standard suppression factor arise generically via multioperator interference effects with the largest enhancements corresponding to regions of parameter space with partial phase alignment between operator contributions.

DOI: 10.1103/4p9z-nd1s

I. INTRODUCTION

Of all of the hitherto observed conservation laws, the apparent protection of baryon number ($\mathcal{B}$) is perhaps the most fragile. Theories of baryogenesis [1–5] require baryon number violation as a Sakharov condition [6]. Similarly for the conservation of lepton number ($\mathcal{L}$), baryon number ($\mathcal{B}$) is conserved in the Standard Model (SM) at the perturbative level due to an accidental global symmetry [7,8]. Both conservation laws are typically not respected when the SM is extended. Away from the perturbative sector, the violation of $\mathcal{B}$ and $\mathcal{L}$ is predicted to occur within the electroweak sector of the SM via sphaleron and instanton processes [9,10] where the quantity ($\mathcal{B} - \mathcal{L}$) is instead conserved. While $\Delta\mathcal{B} = 1$ searches [11–13] dominated attention in early GUT paradigms [14–16], decades of null results motivate complementary paths. Many well-motivated frameworks of physics beyond the SM violate $\mathcal{B}$ by two units [3,17–22].

The most sensitive way to search for a $\Delta\mathcal{B} = 2$ transition is via neutron-antineutron transformations ($n \to \bar{n}$). One method to do this considers an antineutron produced in a long free neutron beam [23–26], while the other utilizes large-volume underground detectors [27–31] to search for intranuclear transitions that lead to matter instability. Each can lead to a highly unique $\bar{n}N$ annihilation signature of multipion final states. While "free" neutron searches are generally inhibited only by energy level splittings δE originating from environmental magnetic fields that can be largely shielded away, the strong nuclear field inhibits the $n \to \bar{n}$ transition. A nucleus-specific parameter, $R = T_b/\tau_f^2$, is generically applied to any experimentally determined intranuclear (bound) lifetime lower limit (T_b) to recover the associated square of the oscillation period for free neutrons (τ_f). Estimations of R are based on phenomenologically mature mean-field/optical potential models assuming a contact interaction and momentum-independent microscopic mixing [32–41]. Typical values of R lie in the range of 10^{22}–10^{23} s^{-1}. Remarkably, given that sensitivities of free and bound searches are determined by wholly different sets of practical constraints, the limits from each method are very similar. The most competitive free or free-equivalent oscillation time lower limits from each method are 0.86×10^8 s [25] from a direct search at the Institut Laue Langevin (ILL), and an inferred limit of 4.7×10^8 s [31] from Super-Kamiokande. With neither method offering dominant sensitivity, it is important that physics, which is not captured in the standard R estimations be considered.

As will be discussed in this paper, scenarios beyond the mean field paradigm used in standard R determinations may change the intranuclear suppression of $n \to \bar{n}$ by multiple orders of magnitude. These include multioperator interference and relaxing the single-step contact approximation. These are relatively unexplored in the literature, particularly with respect to possible cancelations among operator contributions and potential nuclear or kinematic enhancements, unlike, for example, CP-violating operators underlying electric dipole moment (EDM) observables, which are tightly bounded by a broad and complementary suite of measurements (neutron, diamagnetic atoms, paramagnetic molecules, etc.) [42–47]. Neutrinoless double-β decay [48,49], dark-matter–nucleus scattering [50–52], and $\mu \to e$ conversion [53,54] provide further examples of systems for which there is an interplay between short distance and nuclear physics.

Each $n \to \bar{n}$ search method is complementary in the physics that it can elucidate. The observation of $n \to \bar{n}$ at a free neutron experiment provides a powerful probe of Lorentz/CPT-violating backgrounds in the Standard-Model Extension and small Weak Equivalence Principle violations [55,56] to which bound neutron searches are blind. The related $\Delta\mathcal{B} = 2$ process of dinucleon decay is uniquely available via bound nucleon searches [57–59]. Searches for $n \to \bar{n}$ in free space and in various mediums may also give sensitivity to different sets of operator projections.

A. Search status and prospects

Across the experimental landscape, matter stability searches, including bound $n \to \bar{n}$, have become a natural byproduct of large underground neutrino detectors (or, historically, vice versa).

Figure 1, top, shows experimental intranuclear $n \to \bar{n}$ lower exclusion limits versus neutron exposure. Data are given from Fréjus [27], SOUDAN-2 [28], SNO [29], Super-K [30,31], Kamiokande [60], and Irvine-Michigan-Brookhaven (IMB) [61], together with a sensitivity projection from the future DUNE experiment [62].[1] The relevant nuclei are

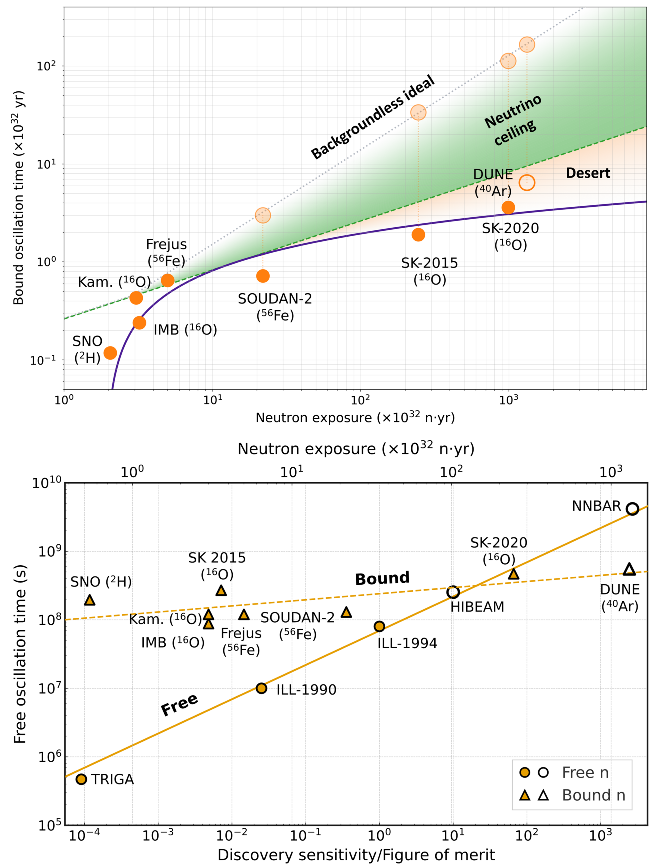

FIG. 1. Top: Intranuclear $n \to \bar{n}$ experimental lower limits from SNO [29], Kamiokande (Kam.) [60], IMB [71], Frejus [27], SOUDAN-2 [28], and Super-Kamiokande (SK-2014 [30], SK-2020 [72]), are shown as closed orange points as a function of neutron exposure; a DUNE sensitivity from the horizontal drift technical design report [62] is shown in an open circle. Open translucent circles are shown for hypothetical ideal sensitivities for large underground detectors assuming a single true event and ∼0 background. Bottom: Free neutron oscillation time as a function of the discovery sensitivity/figure-of-merit from past experiments at TRIGA [24] and the ILL (ILL-1990 [73] and ILL-1994 [25]). Projected sensitivities for the future experiments HIBEAM [74] and NNBAR [75] are also given. Inferred free oscillation time from bound experiments are given for various exposures. Guide lines follow the free and bound data trends.

stated. To guide the eye,[2] the solid purple curve approximately follows the previous limits, with a turnover in sensitivity highlighted for larger volume underground detectors. The dashed green line indicates the ideal statistics-limited trend $\propto \sqrt{\mathrm{exposure}}$, and lies tangent to the solid purple curve, showing the empirical slope change at large exposures—this illustrates the discrepancy between an increase in mass and lowered exclusions due to proportionally lower signal efficiencies and higher neutrino backgrounds. The orange shaded region thus illustrates a

[1]Published projected sensitivities from Hyper-Kamiokande [63] and JUNO [64] have not yet been made.

[2]This curve utilizes only experimentally derived exclusion limits. DUNE sensitivity limits are ignored.

hypothetical "discovery desert," where no discovery of $n \to \bar{n}$ can be convincingly made when dominated by background. Semitransparent "idealized" points are obtained with a TRolke-based[3] construction [65–67]—analogous to the statistical procedure used by Super-Kamiokande [30]—and then fitted to a gray dotted line. The green shaded region thus illustrates the gap between nominal background-limited performance and an idealized zero-background regime—a "Neutrino Ceiling" of sorts. Moving into this region experimentally can excite the possibility of discovery, but is still inevitably limited by at least *some* background. This, of course, is due to the fact that at sufficiently large exposures, atmospheric neutrino interactions can continue to be an irreducible background, imposing practical limits on any sensitivity. This is somewhat analogous to the "neutrino floor" in Weakly Interacting Massive Particle (WIMP) searches [68–70]. This said, unlike the "neutrino floor" case, topological differentiation between the unique intranuclear $\bar{n}N$ annihilation signal and atmospheric backgrounds may be possible using novel and modern analysis methods and could hold the key to breaking this trend, including the use of improved reconstruction algorithms and perhaps direct applications of machine learning and computer vision.

II. CONVERSION OF INTRANUCLEAR RESULTS TO FREE EQUIVALENTS

The so-called quasifree regime for neutrons satisfies $\Delta E t \ll 1$ with $\Delta E \equiv E_n - E_{\bar{n}}$, where E_n ($E_{\bar{n}}$) is the neutron (antineutron) energy and t is the flight time. The two-level amplitude, $A^f(t)$, and probability, P^f, are

$$A^f(t) = -ie^{-i\bar{E}t}\delta m t, \qquad P^f(t) = (\delta m t)^2, \tag{1}$$

where $\bar{E} \equiv (E_n + E_{\bar{n}})/2$. The microscopic mixing, δm, can be written in terms of Wilson coefficients at a scale μ and a hadronic matrix element for a set of operators $\mathcal{O}_i$ computed using lattice QCD [76,77] or more phenomenological approaches [78–80]: $\delta m = \sum_i C_i(\mu)\langle\bar{n}|\mathcal{O}_i(\mu)|n\rangle$. The vacuum oscillation time is defined as $\tau_f = 1/|\delta m|$.

For a neutron bound in a nucleus, taken schematically as a cavity in which the particles experience a constant potential, the effective transition amplitude $A^b(t)$ is given by,

$$A^b(t) = -ie^{-i\bar{E}t}\delta m_{\mathrm{eff}}\frac{1 - e^{-i\Delta E t - \Gamma_{\bar{n}}t/2}}{\Delta E - i\Gamma_{\bar{n}}/2}, \tag{2}$$

and the probability $P^b(t) = |A^b(t)|^2$, where $\Gamma_{\bar{n}}/2$ is the imaginary absorptive part of the optical potential. The mixing for the bound neutron case is defined as

$$\delta m_{\mathrm{eff}} = \sum_{i=1}^{7} C_i^{(9)}(\mu)\langle\bar{n}|O_i^{(9)}(\mu)|n\rangle F_i^{\mathrm{nuc}} \times \left[1 + c_2^{\mathrm{had}}\frac{\langle q^2\rangle_A}{\Lambda_\chi^2} + \cdots\right] \tag{3}$$

$$+ \frac{\langle q^2\rangle_A}{\Lambda_{11}^2}\sum_a C_a^{(11)}(\mu)\langle\bar{n}|O_a^{(11)}(\mu)|n\rangle G_a^{\mathrm{nuc}} + \mathcal{O}\left(\frac{\langle q^2\rangle_A^2}{\Lambda^4}\right), \tag{4}$$

where $\langle q^2\rangle_A \sim p_F^2$ (set by Fermi motion), c_2^{had} parametrizes a hadronic (finite-size/form factor) slope of the $d = 9$ matrix elements, and the explicit q^2/Λ_{11}^2 term captures derivative $d = 11$ effects. The quantities F_i^{nuc} and G_a^{nuc} are nuclear overlap factors encoding many-body/nuclear-structure effects: $F_i^{\mathrm{nuc}} \equiv \int d^3r\psi_{\bar{n}}^*(\mathbf{r})\mathcal{F}_i(\mathbf{r})\psi_n(\mathbf{r})$, where $\mathcal{F}_i(\mathbf{r})$ is a nuclear kernel; an analogous relation exists for G_a^{nuc}.

The R quantity, defined with respect to free and bound oscillation time, can also then be written,

$$R = \frac{T_b}{\tau_f^2} = \frac{\Delta E^2 + (\Gamma_{\bar{n}}/2)^2}{\Gamma_{\bar{n}}}\frac{(\delta m)^2}{(\delta m_{\mathrm{eff}})^2}. \tag{5}$$

In conventional analyses, R is evaluated within a mean-field/optical-potential framework. The seven $d = 9$ operators identified as providing $n \to \bar{n}$ [81] are taken as coherent with no momentum dependence of the mixing. It is assumed that in an effective field theory (EFT) with a clear scale hierarchy (nucleon size < internucleon spacing), the short-distance $\Delta\mathcal{B} = 2$ physics factorizes with the universal quadratic nucleon operator $n^T C n$ dominating with medium-dependent effects suppressed. This is hereafter referred to as the standard or baseline picture.

Within the standard picture of R, determinations of R carry a model dependence from optical potentials, annihilation widths, and nuclear structure. Quantifying these effects requires consistent hadronic inputs and many-body methods; some assessments span up to around 50% [21].

We stress that the equation in Eq. (3) is factorized in the sense that the six-quark operators are matched first to neutron-antineutron matrix elements, and then placed in the nuclear medium by means of overlap factors. In a more general treatment of the hadronic matching, the $\Delta B = 2$ operators could induce other transitions with multinucleon and/or nucleon-pion states on the left-hand side, such as, for example, $\langle NN|O|0\rangle$ or $\langle NN\pi|O|N\rangle$ etc. Such terms arise naturally within a hadronic matching and depend significantly on the chirality and spin-isospin structure of the operators. Inclusion of such matrix elements would not

[3] For each experiment we assume a single signal event is present with a 50% signal efficiency *a la* SNO and ILL, alongside a background of ~0.01 neutrino events. The signal efficiency and background rate errors are taken from the experimental values, if available. For each idealized limit, 1000 pseudoexperiments are performed from Poissonian throws of the observed single event, and the median of the limit results from these pseudoexperiments is shown in each translucent point.

restore universality of the in-medium suppression factor; on the contrary, it would bring additional operator-dependent nuclear structures, further reinforcing the idea that the mapping between free and bound neutron transitions is scenario dependent.

III. BEYOND THE BASELINE: IN-MEDIUM REWEIGHTING AND MULTIOPERATOR INTERFERENCE

Different operators carry different chiral and color-spin structures (e.g., $Q_L Q_L Q_L Q_L d_R d_R$ vs $u_R d_R u_R d_R d_R d_R$), which transform differently under chiral rotations. In vacuum these differences can be immaterial if they contribute coherently to the same neutron-antineutron bilinear. In nuclear matter, however, chiral symmetry is explicitly and spontaneously broken; pion exchange, tensor forces, and spin-isospin correlations couple differently to left- and right-handed quark bilinears and to distinct color contractions. As a result, the in-medium renormalization of operator classes generally differs, leading to operator-dependent reweighting of the matrix elements even if the same operators add coherently in vacuum. In our notation this appears as an operator dependence in F_i^{nuc} and in analogous factors for other operators [21,39,82–84].

Second, empirical evidence for medium modifications of quark-level structure comes from the EMC effect, which shows $\mathcal{O}(10\% - 20\%)$ differences in quark momentum distributions between bound and free nucleons [85]. If such linear-response modifications are present at high Q^2, it is not *a priori* justified to assume that highly nonlinear six-quark operators experience no medium reweighting.

Third, the nuclear environment exhibits short-range correlations (SRCs) that strongly distort the high-momentum tail of the nucleon momentum distribution. Electron-scattering measurements indicate that these tails are generated by short-range NN dynamics rather than a mean-field picture, with np pairs dominating over pp and nn pairs [86,87]. Such SRCs modify the overlap of six-quark operators with the relevant nuclear wave function components, again implying operator-dependent F_i^{nuc}.

Finally, nuclear matrix elements can receive multinucleon contributions: a six-quark operator may involve quarks residing in different, spatially separated nucleons. Although the mean internucleon distance (∼1–2 fm) exceeds the hadronic scale, Pauli blocking, scalar mean fields, and nucleon overlap alter short-distance nucleon structure and thus the effective matching of quark operators onto hadronic/nuclear degrees of freedom.

A. Multioperator interference

Taken together, these effects described above imply that (i) the relative in-medium weights of different $\Delta\mathcal{B} = 2$ operators can in general differ from their vacuum values, and (ii) constructive or destructive multioperator interference in nuclei can arise even when such interference is absent for free neutrons. In the one-body amplitude, coherent interference is generic among the momentum-independent dim-9 and dim-11 pieces and the derivative contributions (both UV dim-11 and hadronic/in medium). Predicting cancelations or enhancements therefore requires knowledge of Wilson coefficients (magnitudes and phases) and operator-resolved in-medium matrix elements.

Much theoretical work remains to be done in this area. However, models can be identified for which interference would be expected and the sensitivity of R to interference within a given scenario estimated.

1. Left-right symmetry and multiple operators with $\Delta(\mathcal{B}-\mathcal{L})=2$

The first interesting gauge theory where $n \to \bar{n}$ transitions were predicted at observable rates was left-right symmetric theory with quark-lepton unification [17]. It is shown that this model gives four kinds of independent operators with the dimension $d = 9$, in which case there will definitely be different relative values for their contributions to oscillation versus nuclear decay. For example, in this model the source of the $\Delta\mathcal{B} = 2$ interaction is the four $SU(4)_C$ 10-plet Higgs field of type $\epsilon^{aceg}\epsilon^{bdfh}\vec{\Delta}_{R,ab} \cdot \vec{\Delta}_{R,cd}\vec{\Delta}_{R,ef} \cdot \vec{\Delta}_{R,gh}$ and $\epsilon^{aceg}\epsilon^{bdfh}\vec{\Delta}_{L,ab} \cdot \vec{\Delta}_{L,cd}\vec{\Delta}_{R,ef} \cdot \vec{\Delta}_{R,gh}$ where $a,\ldots h$ are the $\mathrm{SU}(4)_C$ indices and vector signs correspond to $\mathrm{SU}(2)_{L,R}$ groups. When the $\Delta_{R,44}$ field acquires a vacuum expectation value (VEV), v_{BL}, they give rise to cubic coupled color sextet product operators of type $v_{BL}\epsilon^{ikm}\epsilon^{jln}\Delta_{R,ij}\Delta_{R,kl}\Delta_{R,mn}$ and $v_{BL}\epsilon^{ikm}\epsilon^{jln}\Delta_{L,ij}\Delta_{L,kl}\Delta_{R,mn}$. Couplings of these scalars to quarks give rise to the following operators that violate $B - L$ by two units,

$$\begin{aligned}\Bigg[&\frac{\lambda_R v_{BL}}{M_{\Delta_R}^6} u_R d_R u_R d_R d_R d_R + \frac{\lambda_R v_{BL}}{M_{\Delta_R}^6} d_R d_R u_R u_R d_R d_R \\ &+ \frac{\lambda_L v_{BL}}{M_{\Delta_L}^4 M_{\Delta_R}^2} u_L d_L u_L d_L d_R d_R \\ &+ \frac{\lambda_L v_{BL}}{M_{\Delta_L}^4 M_{\Delta_R}^2} u_L u_L d_L d_L d_R d_R \Bigg] T_S \end{aligned} \tag{6}$$

where $T_S = \epsilon_{cae}\epsilon_{dbf} + \epsilon_{cbf}\epsilon_{dae} + \epsilon_{cbe}\epsilon_{daf} + \epsilon_{caf}\epsilon_{dbe}$, as given in the next Subsection. As a result, there are two independent RRR operators, and two LLR, which appear together. The transition and decay operators will therefore, in general, give different contributions, leading to the kind of effects being discussed here. A similar multiple operator structure also arises in left-right models in five dimensions [88].

2. Neutron oscillations from R-parity violation in SUSY

In supersymmetric models with R-parity violation (RPV) [20], the superpotential term,

$$W_{\mathrm{RPV}} \supset \frac{1}{2}\lambda''_{ijk} U_i^c D_j^c D_k^c \tag{7}$$

violates baryon number by one unit ($\Delta B = 1$). Here, U_i^c and D_j^c denote the right-handed up- and down-type quark superfields of generation i and j, respectively, and λ''_{ijk} is a dimensionless complex coupling controlling the strength of the baryon-number-violating interaction. The factor $1/2$ accounts for the antisymmetry of the color contraction between the two down-type superfields. Two insertions of this vertex, connected by virtual gluino exchange, generate $\Delta B = 2$ six-quark operators in the low-energy effective theory [22]. Since the couplings λ''_{ijk} are independent parameters, different color and flavor contractions produce a generic linear combination of operators in the neutron–antineutron EFT basis. For example, for some choice of parameters, two operators that are induced after SUSY breaking are,

$$\begin{aligned}\mathcal{O}_1 &= u_R^a C d_R^b u_R^c C d_R^d d_R^e C d_R^f T^s_{abcdef},\\ \mathcal{O}_2 &= d_R^a C u_R^b d_L^c C d_L^d u_R^e C d_R^f T^s_{abcdef},\end{aligned} \tag{8}$$

where C is the charge conjugation matrix and $T^s_{abcdef} = \epsilon_{cae}\epsilon_{dbf} + \epsilon_{cbf}\epsilon_{dae} + \epsilon_{cbe}\epsilon_{daf} + \epsilon_{caf}\epsilon_{dbe}$ [89]. Both terms arise from down squark exchange [22]. Prior to gauge symmetry breaking, these operators involve two different down flavors but once flavor mixings are included via SUSY breaking, the "flavor diagonal" $n \to \bar{n}$ operator emerges.

Thus, operator interference of the type studied here can arise in RPV SUSY. In the EFT basis, the effective dimension-9 operator coefficients are related to the squark and gluino masses and SUSY breaking parameters Δ_{LR} and δ_{RR} as follows:

$$C_{\mathrm{RPV}} \sim \frac{\lambda''^2 \delta_{\mathrm{SUSY}}}{m_{\tilde{q}}^4 m_{\lambda_g}}, \tag{9}$$

where $\tilde{q}$ and λ_g, respectively, denote the squark and gluino masses and δ_{SUSY} involves the SUSY breaking parameters (see [22] for detailed expressions for the SUSY breaking parameters).

IV. MONTE CARLO ANALYSIS OF OPERATOR INTERFERENCE IN RPV SUSY

In order to quantify in-medium effects on neutron–antineutron oscillations, we perform a Monte Carlo study within a benchmark R-parity-violating supersymmetric framework. The analysis incorporates both nuclear dressing and the complex phases of the Wilson coefficients. This approach allows us to examine how these effects modify the in-medium single-operator transition rate and to identify parameter regions that lead to constructive or destructive interference.

The Wilson coefficients from the RPV SUSY scaling are taken as $C_1 = \frac{\lambda''_{113}\delta_{RR}\lambda''_{112}\delta_{RR}}{m_{\tilde{q}_d}^4 m_{\tilde{g}}}$ and $C_2 = \frac{(\lambda''_{113}\delta_{LR})^2}{m_{\tilde{q}_d}^4 m_{\tilde{g}}} e^{i(\phi_{C_2}-\phi_{C_1})}$, where ϕ_i is the complex phase of the ith coefficient and δ's are SUSY breaking contributions. In this study, C_1 is taken real ($\phi_1 = 0$), and C_2 is allowed to vary in phase relative to C_1: $\phi_{C_2} - \phi_{C_1} \in [0, 2\pi]$. The vacuum matrix elements are fixed at $M_{f_i} = [100.0, 100.0]$ MeV for $i = 1,\ 2$, and the in-medium matrix elements include nuclear dressing via $M_{a_i} = F_i^{\mathrm{nuc}} M_{f_i}$. The RPV SUSY benchmark parameters are $m_{\tilde{q}_d} = 6$ TeV, $m_{\tilde{g}} = 9$ TeV, $\lambda''_{113}\delta_{RR} = 0.6$, $\lambda''_{112}\delta_{RR} = 0.4$, and $\lambda''_{113}\delta_{LR} = 0.6$. This makes it explicit that C_1 is a cross-term involving two different couplings, while C_2 is a single-coupling squared term.

With the benchmark choice of superpartner masses and couplings, the vacuum oscillation lifetime is $\tau_f = 1/|\delta m|$, with $\delta m = \sum_i C_i M_{f_i}$ For the baseline values this gives $\tau_f \simeq 1.92 \times 10^{11}$ s. More generally, the oscillation time depends on the magnitude and relative phase of the Wilson coefficients as $|\delta m| = |C_1 M_{f_1} + C_2 M_{f_2} e^{i(\phi_{C_2}-\phi_{C_1})}|$.

To explore the effects of nuclear dressing and operator interference, a Monte Carlo scan of $N = 10^7$ random parameter points was performed, varying $|F_1^{\mathrm{nuc}}| \in [1.05, 1.30]$, $|F_2^{\mathrm{nuc}}| \in [1.10, 1.60]$, and $\phi_{C_2} - \phi_{C_1} \in [0, 2\pi]$. For each sampled point, the normalized rate R/R_{std} is computed relative to the single-operator reference.

From the ensemble of Monte Carlo samples, we computed the survival probability $P(R/R_{\mathrm{std}} > x) = 1 - \mathrm{CDF}(R/R_{\mathrm{std}})$, where CDF denotes the cumulative distribution function of the normalized rate. This function denotes the fraction of Monte Carlo samples yielding a normalized rate greater than x, i.e., the volume fraction of parameter space where the in-medium enhancement exceeds x times the standard case, as shown in Fig. 2. Most samples cluster around moderate values, typically within one order of magnitude of the

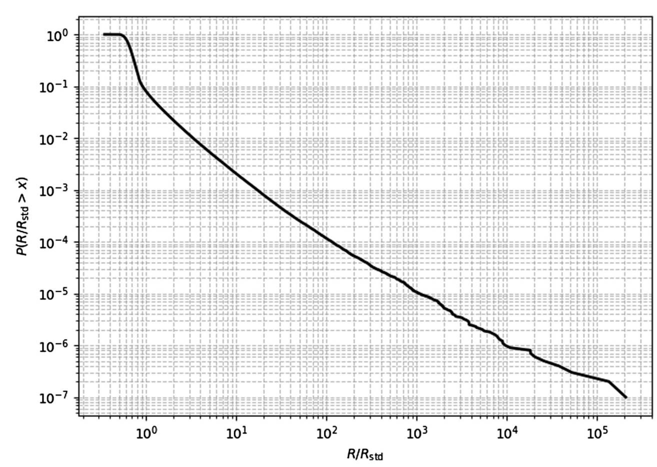

FIG. 2. Survival probability $P(R/R_{\mathrm{std}} > x)$ as a function of R/R_{std} computed from 10^7 Monte Carlo samples.

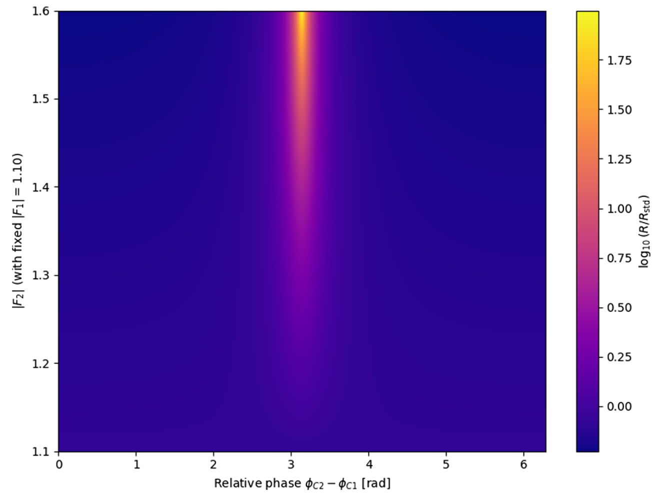

FIG. 3. Heatmap of $\log_{10}(R/R_{\rm std})$ as a function of the relative Wilson coefficient phase $\phi_{C_2}-\phi_{C_1}$ and $|F_2|$, for fixed $|F_1| = 1.1$.

standard rate, while a small fraction of points form a long tail reaching up to $\mathcal{O}(10^3)$, with only a handful of points extending beyond 10^4. Although the fraction of points leading to strong suppression is significantly smaller, such regions of parameter space are not negligible given that the relative complex phases of the Wilson coefficients are *a priori* unknown. Even small phase variations can therefore induce cancelations that reduce the effective in-medium oscillation rate by several orders of magnitude.

Figure 3 shows a two-dimensional heatmap of $R/R_{\rm std}$ as a function of the relative phase $\phi_{C_2}-\phi_{C_1} \in [0, 2\pi]$ and $|F_2|$ for fixed $|F_1|$, highlighting regions of constructive and destructive interference. The scan demonstrates that interference and nuclear dressing can enhance or suppress the n–$\bar{n}$ transition rate by several orders of magnitude, with constructive interference occurring for small relative phases, while amplitude-level destructive interference aligns near $\phi_{C_2}-\phi_{C_1} \approx \pi$ and is amplified for large $|F_2^{\rm nuc}|$. The full dynamic range of this effect extends beyond what is visible in the color scale of the heatmap, as extreme enhancements correspond to a very small fraction of the sampled parameter space.

The survival probability shown in Fig. 2 can also be interpreted as a quantitative measure of the degree of parameter alignment required to obtain a given enhancement. In particular, the figure directly shows the fraction of the multioperator parameter space that produces deviations from the standard suppression factor under the scan prior. Moderate deviations arise generically, while the largest enhancements correspond to smaller but still finite and continuous regions of parameter space. This behavior is characteristic of interference between contributions of comparable magnitude: achieving large effects requires a degree of alignment between amplitudes, but not extreme hierarchies among the underlying parameters. In this sense, Fig. 2 provides a direct quantitative characterization of the level of parameter alignment relevant for the observable R.

V. TWO STEP $n \to \bar{n}$ PROCESS

The $n \to \bar{n}$ transition can occur in a two-step process in hidden sector scenarios [90,91]. In Ref. [90], a neutron converts into a sterile neutron n', which subsequently converts into an antineutron [90].

Following Ref. [90], a two-step process, $n \to n' \to \bar{n}$, is considered in which the three levels are degenerate in vacuum, $E_n = E_{n'} = E_{\bar{n}}$. This approach can be applied for a range of magnetic field intervals in order to match equivalent fields in a hidden sector. Here, the case $B < 10$ nT is considered. This corresponds to the field values needed to achieve the quasifree condition in a traditional free $n \to \bar{n}$ search with beam neutrons [92].

For quasifree neutrons, time-dependent perturbation theory gives the probability for short times,

$$\mathcal{P}_f^{(2)}(t) = \frac{|\varepsilon_{nn'}\varepsilon_{n'\bar{n}}|^2}{4} t^4. \tag{10}$$

In this case, the free-beam probability grows as t^4, not t^2 as in the baseline one-step case. The appropriate free figure-of-merit and number of $\bar{n}$ annihilations at a beam experiment are, respectively,

$$F^{(2)} \equiv \frac{N\langle t^4\rangle}{4} \tag{11}$$

and

$$Y_{\rm f}^{(2)} = |\varepsilon_{nn'}\varepsilon_{n'\bar{n}}|^2 F_{\rm f}^{(2)}. \tag{12}$$

Here, N is the accumulated number of free neutrons in the run and t is the neutron flight time determined by the spectrometer geometry [25,73].

Inside nuclei the sterile level is detuned by the neutron mean field, while the $\bar{n}$ experiences a complex optical potential. In the optical–potential formalism [21,33,93] the two–step intranuclear transition rate per bound neutron is

$$T_b^{(2)} = \frac{\Gamma|\varepsilon_{nn'}\varepsilon_{n'\bar{n}}|^2}{\Delta_{n'}^2[\Delta^2 + (\Gamma/2)^2]}, \tag{13}$$

where $\Delta = (E_n - E_{\bar{n}})$ is the energy splitting of n and $\bar{n}$ in the medium, $\Gamma \equiv -2\,{\rm Im}\,E_{\bar{n}}$ is the absorptive width of $\bar{n}$ in the medium, and $\Delta_{n'} \equiv E_n - E_{n'}$ is the in-medium nondegeneracy of the sterile neutron n' with ($\Delta_{n'} \equiv E_n - E_{n'} \sim \mathcal{O}(5\text{–}60)$) MeV depending on peripherality/surface weighting [93]. For a detector with a total number of bound neutrons N_b and live time T, the expected intranuclear yield is

$$Y_{\mathrm{b}}^{(2)} = |\varepsilon_{nn'}\varepsilon_{n'\bar{n}}|^2 \frac{\Gamma}{\Delta_{n'}^2[\Delta^2 + (\Gamma/2)^2]}(N_b T). \quad (14)$$

A representative one-year run at the ILL corresponds to $N \sim 2 \times 10^{18}$ and $\langle t^4 \rangle \sim 10^{-4}$ s^4 [25]. Taking Super–Kamiokande as an example of a bound experiment, $(N_b T)_{\mathrm{b}} \sim (6 \times 10^{33}) \times (1\ \mathrm{yr}) \sim 1.9 \times 10^{41}$ neutron − s for 22.5 kt fiducial water over one year [31]. For optical-model inputs, the following values are set: $\Delta \sim 60$ MeV and $\Gamma \sim 200$ MeV [21,33,93], with a surface-weighted sterile detuning of $\Delta_{n'} = 5$ MeV. The ratio of expected yields can be estimated,

$$\frac{Y_{\mathrm{f}}^{(2)}}{Y_{\mathrm{b}}^{(2)}} = \frac{F_{\mathrm{f}}^{(2)}}{(N_b T)} \frac{\Delta_{n'}^2[\Delta^2 + (\Gamma/2)^2]}{\Gamma} \sim 1.8 \times 10^{39}. \quad (15)$$

The above example scenario illustrates how a standard low-field free neutron experiment can be sensitive to $n \to \bar{n}$ transitions despite bound neutron searches being blind to them.

This class of constructions should be understood as a generic realization of multistep oscillation dynamics in the presence of intermediate sterile or hidden-sector states, rather than as a model-specific or *ad hoc* scenario. Such mechanisms appear naturally in several well-studied frameworks, including mirror-neutron models and extradimensional theories with Kaluza-Klein fermions, and represent consistent ultraviolet completions in which neutron-antineutron mixing proceeds via an intermediate propagation stage. From the effective field theory perspective adopted here, they are therefore not distinguished in principle from other UV completions that generate $\Delta B = 2$ operators, and are included as a legitimate realization of the general oscillation structure.

A. Naturalness and phase alignment

Large variations of R arise from the coherent superposition of contributions from different $\Delta B = 2$ operators in the in-medium amplitude. Because these contributions enter with complex Wilson coefficients and nonproportional nuclear matrix elements, the observable depends on ratios of coherent sums of operator contributions. Interference can therefore lead to both suppressions and enhancements over extended regions of parameter space without requiring any hierarchy among operator coefficients.

Enhancements are most pronounced when multiple operator contributions have comparable magnitude and relative phases close to π, producing partial cancelations in the in-medium amplitude while leaving the free amplitude largely unaffected. Moderate enhancements already appear generically once several operators contribute with similar size. In our scans, enhancement factors of order 10^2 arise for mild phase alignment, while larger values up to 10^4 occur in the tail of the distribution and correspond to stronger, but still continuous, alignment in the space of Wilson coefficients.

This mechanism does not rely on extreme parameter hierarchies. Existing estimates of neutron–antineutron matrix elements indicate that different operators can naturally differ by factors of order unity, e.g. $\langle O_2 \rangle / \langle O_1 \rangle \sim 2$ in the classic analysis of Rao and Shrock [82]. Large effects therefore arise once nuclear overlap factors are also comparable and the relative phase between contributions approaches π.

The qualitative structure of these enhancements is generic to any framework in which multiple operators contribute coherently with nontrivial relative phases and is not specific to the assumptions used in the numerical scan.

VI. CONCLUSIONS

The mapping of bound-neutron limits to free-neutron constraints for $n \to \bar{n}$ is traditionally made with a nucleus-specific conversion factor, estimated with a mean field theory approach that is assumed to be valid for all $n \to \bar{n}$ scenarios. However, multioperator interference and multistep processes can lead to variations in R of orders of magnitude with respect to the standard approach. Depending on the theory scenario, either free or bound neutron searches can deliver higher sensitivity. This argues for a broad program in which high-sensitivity searches are made using both methods. Furthermore, in analogy to comparable systems (e.g., EDM, neutrinoless double beta decay), there is a need for a phenomenology program that integrates all available $\Delta B = 2$ information (free and bound $n \to \bar{n}$, and dinucleon-decay searches) into a single, operator-based global analysis.

ACKNOWLEDGMENTS

We gratefully acknowledge helpful discussions with Mike Snow, Arkady Vainshtein, and Jean-Marc Richard. J. L. B. would also like to thank Daisy Kalra, Linyan Wan, and Tyler Stokes for TRolke starting codes and associated discussion over many years. B. M. and D. M. gratefully acknowledge support from the Swedish Research Council.

DATA AVAILABILITY

The data are not publicly available. The data are available from the authors upon reasonable request.

[1] A. Riotto and M. Trodden, Annu. Rev. Nucl. Part. Sci. **49**, 35 (1999).
[2] M. Dine and A. Kusenko, Rev. Mod. Phys. **76**, 1 (2003).
[3] K. Babu, R. Mohapatra, and S. Nasri, Phys. Rev. Lett. **97**, 131301 (2006).
[4] L. Canetti, M. Drewes, and M. Shaposhnikov, New J. Phys. **14**, 095012 (2012).
[5] K. S. Babu, P. S. Bhupal Dev, E. C. F. S. Fortes, and R. N. Mohapatra, Phys. Rev. D **87**, 115019 (2013).
[6] A. D. Sakharov, Pis'ma Zh. Eksp. Teor. Fiz. **5**, 32 (1967).
[7] S. Weinberg, Phys. Rev. Lett. **43**, 1566 (1979).
[8] F. Wilczek and A. Zee, Phys. Rev. Lett. **43**, 1571 (1979).
[9] G. 't Hooft, Phys. Rev. Lett. **37**, 8 (1976).
[10] V. A. Kuzmin, V. A. Rubakov, and M. E. Shaposhnikov, Phys. Lett. **155B**, 36 (1985).
[11] K. Abe *et al.* (Super-Kamiokande Collaboration), Phys. Rev. D **95**, 012004 (2017).
[12] K. Abe *et al.* (Super-Kamiokande Collaboration), Phys. Rev. D **90**, 072005 (2014).
[13] K. S. Hirata *et al.* (Kamiokande Collaboration), Phys. Lett. B **220**, 308 (1989).
[14] H. Georgi and S. L. Glashow, Phys. Rev. Lett. **32**, 438 (1974).
[15] P. Langacker, Phys. Rep. **72**, 185 (1981).
[16] S. Navas *et al.* (Particle Data Group), Phys. Rev. D **110**, 030001 (2024).
[17] R. N. Mohapatra and R. E. Marshak, Phys. Rev. Lett. **44**, 1316 (1980); **44**, 1644 (1980).
[18] R. N. Mohapatra and G. Senjanovic, Phys. Rev. D **23**, 165 (1981).
[19] S. Nussinov and R. Shrock, Phys. Rev. Lett. **88**, 161601 (2002).
[20] R. Barbier *et al.*, Phys. Rep. **420**, 1 (2005).
[21] D. G. Phillips, W. M. Snow, K. Babu, S. Banerjee, D. V. Baxter, Z. Berezhiani *et al.*, Phys. Rep. **612**, 1 (2016).
[22] L. Calibbi, G. Ferretti, D. Milstead, C. Petersson, and R. Pöttgen, J. High Energy Phys. 05 (2016) 144; 10 (2017) 195 (E).
[23] G. Fidecaro, M. Fidecaro, L. Lanceri *et al.*, Phys. Lett. **156B**, 122 (1985).
[24] G. Bressi, E. Calligarich, M. Cambiaghi *et al.*, Il Nuovo Cimento A **103**, 731 (1990).
[25] M. Baldo-Ceolin *et al.*, Z. Phys. C **63**, 409 (1994).
[26] A. Addazi *et al.*, J. Phys. G **48**, 070501 (2021).
[27] C. Berger, M. Fröhlich, H. Mönch *et al.* (Fréjus Collaboration), Phys. Lett. B **240**, 237 (1990).
[28] J. Chung, W. W. M. Allison, G. J. Alner *et al.* (Soudan 2 Collaboration), Phys. Rev. D **66**, 032004 (2002).
[29] B. Aharmim *et al.* (SNO Collaboration), Phys. Rev. D **96**, 092005 (2017).
[30] K. Abe and *et al.* (Super-Kamiokande Collaboration), Phys. Rev. D **91**, 072006 (2015).
[31] K. Abe and *et al.* (Super-Kamiokande Collaboration), Phys. Rev. D **103**, 012008 (2021).
[32] W. M. Alberico, A. Bottino, and A. Molinari, Phys. Lett. **114B**, 266 (1982).
[33] C. B. Dover, A. Gal, and J. M. Richard, Phys. Rev. D **27**, 1090 (1983).
[34] W. M. Alberico, J. Bernabeu, A. Bottino, and A. Molinari, Nucl. Phys. **A429**, 445 (1984).
[35] C. B. Dover, A. Gal, and J. M. Richard, Phys. Rev. C **31**, 1423 (1985).
[36] C. B. Dover, A. Gal, and J. M. Richard, Nucl. Instrum. Methods Phys. Res., Sect. A **284**, 13 (1989).
[37] W. M. Alberico, A. De Pace, and M. Pignone, Nucl. Phys. **A523**, 488 (1991).
[38] J. Hufner and B. Z. Kopeliovich, Mod. Phys. Lett. A **13**, 2385 (1998).
[39] E. Friedman and A. Gal, Phys. Rev. D **78**, 016002 (2008).
[40] J. L. Barrow, E. S. Golubeva, E. Paryev, and J.-M. Richard, Phys. Rev. C **105**, 065501 (2022).
[41] J. L. Barrow, E. S. Golubeva, E. Paryev, and J.-M. Richard, Phys. Rev. D **101**, 036008 (2020).
[42] M. Pospelov and A. Ritz, Ann. Phys. (Amsterdam) **318**, 119 (2005).
[43] J. Engel, M. J. Ramsey-Musolf, and U. van Kolck, Prog. Part. Nucl. Phys. **71**, 21 (2013).
[44] C.-P. Liu, J. Engel, C. M. Maekawa, T. N. Mukhopadhyay, B. K. Sahoo, and M. J. Ramsey-Musolf, Phys. Rev. C **76**, 035503 (2007).
[45] V. V. Flambaum and J. S. M. Ginges, Phys. Rev. A **65**, 032113 (2002).
[46] J. de Vries, R. Higa, C.-P. Liu, E. Mereghetti, I. Stetcu, R. G. E. Timmermans, and U. van Kolck, Phys. Rev. C **84**, 065501 (2011).
[47] J. Bsaisou, J. de Vries, C. Hanhart, S. Liebig, U.-G. Meißner, D. Minossi, A. Nogga, and A. Wirzba, J. High Energy Phys. 03 (2015) 104.
[48] J. Engel and J. Menéndez, Rep. Prog. Phys. **80**, 046301 (2017).
[49] V. Cirigliano, W. Dekens, J. de Vries, M. L. Graesser, and E. Mereghetti, J. High Energy Phys. 12 (2018) 097.
[50] A. L. Fitzpatrick, W. Haxton, E. Katz, N. Lubbers, and Y. Xu, J. Cosmol. Astropart. Phys. 02 (2013) 004.
[51] N. Anand, A. L. Fitzpatrick, and W. C. Haxton, Phys. Rev. C **89**, 065501 (2014).
[52] K. Schneck *et al.* (SuperCDMS Collaboration), Phys. Rev. D **91**, 092004 (2015).
[53] L. Calibbi and G. Signorelli, Riv. Nuovo Cimento **41**, 71 (2018).
[54] R. Kitano, M. Koike, and Y. Okada, Phys. Rev. D **66**, 096002 (2002).
[55] K. S. Babu and R. N. Mohapatra, Phys. Rev. D **91**, 096009 (2015).
[56] A. Addazi, Z. Berezhiani, and Y. Kamyshkov, Eur. Phys. J. C **77**, 301 (2017).
[57] M. Litos *et al.* (Super-Kamiokande Collaboration), Phys. Rev. Lett. **112**, 131803 (2014).
[58] J. Gustafson *et al.* (Super-Kamiokande Collaboration), Phys. Rev. D **91**, 072009 (2015).
[59] V. Takhistov *et al.* (Super-Kamiokande Collaboration), Phys. Rev. Lett. **115**, 121803 (2015).
[60] M. Takita, K. Arisaka, T. Kajita, T. Kifune, M. Koshiba, K. Miyano, M. Nakahata, Y. Oyama, N. Sato, T. Suda, A. Suzuki, K. Takahashi, and Y. Totsuka (Kamiokande Collaboration), Phys. Rev. D **34**, 902 (1986).
[61] T. W. Jones *et al.* (Irvine–Michigan–Brookhaven (IMB) Collaboration), Phys. Rev. Lett. **52**, 720 (1984).
[62] B. Abi *et al.* (DUNE Collaboration), Deep underground neutrino experiment (DUNE), far detector technical design

report, Volume II: DUNE Physics, Technical Report, 2020, arXiv:2002.03005.

[63] K. Abe *et al.* (Hyper-Kamiokande Proto-Collaboration), Hyper-Kamiokande Design Report, Technical Report, 2018, v2arXiv:1805.04163.

[64] A. Abusleme *et al.* (JUNO Collaboration), Prog. Part. Nucl. Phys. **123**, 103927 (2022).

[65] W. A. Rolke, A. M. López, and J. Conrad, Nucl. Instrum. Methods Phys. Res., Sect. A **551**, 493 (2005).

[66] W. A. Rolke and A. M. López, Nucl. Instrum. Methods Phys. Res., Sect. A **458**, 745 (2001).

[67] J. Lundberg, J. Conrad, W. Rolke, and A. López, Comput. Phys. Commun. **181**, 683 (2010).

[68] J. Monroe and P. Fisher, Phys. Rev. D **76**, 033007 (2007).

[69] J. Billard, L. Strigari, and E. Figueroa-Feliciano, Phys. Rev. D **89**, 023524 (2014).

[70] F. Ruppin, J. Billard, E. Figueroa-Feliciano, and L. Strigari, Phys. Rev. D **90**, 083510 (2014).

[71] T. W. Jones, R. M. Bionta, G. Blewitt *et al.* (IMB Collaboration), Phys. Rev. Lett. **52**, 720 (1984).

[72] K. Abe *et al.* (Super-Kamiokande Collaboration), Phys. Rev. D **103**, 012008 (2021).

[73] M. Baldo-Ceolin, P. Benetti, T. Bitter *et al.*, Phys. Lett. B **236**, 95 (1990).

[74] V. Santoro *et al.*, J. Phys. G **52**, 040501 (2025).

[75] V. Santoro *et al.*, J. Neutron Res. **25**, 315 (2024).

[76] E. Rinaldi, S. Syritsyn, M. L. Wagman, M. I. Buchoff, C. Schroeder, and J. Wasem, Phys. Rev. Lett. **122**, 162001 (2019).

[77] E. Rinaldi, S. Syritsyn, M. L. Wagman, M. I. Buchoff, C. Schroeder, and J. Wasem, Phys. Rev. D **99**, 074510 (2019).

[78] A. Chodos, R. L. Jaffe, K. Johnson, C. B. Thorn, and V. F. Weisskopf, Phys. Rev. D **9**, 3471 (1974).

[79] A. Chodos, R. L. Jaffe, K. Johnson, and C. B. Thorn, Phys. Rev. D **10**, 2599 (1974).

[80] A. Chodos and C. B. Thorn, Phys. Lett. B **53**, 359 (1974).

[81] Z. Berezhiani and A. Vainshtein, Phys. Lett. B **788**, 58 (2019).

[82] S. Rao and R. E. Shrock, Phys. Lett. **116B**, 238 (1982).

[83] S. Rao and R. E. Shrock, Nucl. Phys. **B232**, 143 (1984).

[84] M. I. Buchoff and M. L. Wagman, Phys. Rev. D **93**, 016005 (2016).

[85] A. W. Thomas, Int. J. Mod. Phys. E **27**, 1840001 (2019).

[86] J. Arrington, D. W. Higinbotham, G. Rosner, and M. Weinstein, Prog. Part. Nucl. Phys. **67**, 898 (2012).

[87] J. Arrington, N. Fomin, and A. Schmidt, Annu. Rev. Nucl. Part. Sci. **72**, 307 (2022).

[88] S. Girmohanta and R. Shrock, Phys. Rev. D **101**, 095012 (2020).

[89] S. Rao and R. E. Shrock, Phys. Lett. **116B**, 238 (1982).

[90] Z. Berezhiani, Eur. Phys. J. C **81**, 33 (2021).

[91] G. Dvali, M. Ettengruber, and A. Stuhlfauth, Phys. Rev. D **109**, 055046 (2024).

[92] E. D. Davis and A. R. Young, Phys. Rev. D **95**, 036004 (2017).

[93] E. Friedman and A. Gal, Phys. Rev. D **78**, 016002 (2008).